VYSOKÉ UČENÍ TECHNICKÉ V BRNĚ
BRNO UNIVERSITY OF TECHNOLOGY

FAKULTA STROJNÍHO INŽENÝRSTVÍ
FACULTY OF MECHANICAL ENGINEERING

ÚSTAV FYZIKÁLNÍHO INŽENÝRSTVÍ
INSTITUTE OF PHYSICAL ENGINEERING

KOMPARATIVNÍ SPEKTRÁLNÍ ANALÝZA METODAMI ESA–LEIS A TOF–LEIS
COMPARATIVE SPECTRAL ANALYSIS BY ESA–LEIS AND TOF–LEIS METHODS

BAKALÁŘSKÁ PRÁCE
BACHELOR'S THESIS

AUTOR PRÁCE
AUTHOR
Tomáš Strapko

VEDOUCÍ PRÁCE
SUPERVISOR
Ing. Petr Bábor, Ph.D.

BRNO 2017

VYSOKÉ UČENÍ TECHNICKÉ V BRNĚ
FAKULTA STROJNÍHO INŽENÝRSTVÍ

Zadání bakalářské práce

Ústav:	Ústav fyzikálního inženýrství
Student:	**Tomáš Strapko**
Studijní program:	Aplikované vědy v inženýrství
Studijní obor:	Fyzikální inženýrství a nanotechnologie
Vedoucí práce:	**Ing. Petr Bábor, Ph.D.**
Akademický rok:	2016/17

Ředitel ústavu Vám v souladu se zákonem č.111/1998 o vysokých školách a se Studijním a zkušebním řádem VUT v Brně určuje následující téma bakalářské práce:

Komparativní spektrální analýza metodami ESA–LEIS a TOF–LEIS

Stručná charakteristika problematiky úkolu:

Nízkoenergiový rozptyl iontů (Low Energy Ion Scattering – LEIS) je často využíván při analýze čistoty povrchů a hloubkovém profilování tenkých vrstev. Pomocí měření energie rozptýleného iontu lze provést prvkovou analýzu studovaných povrchů. Při kolizi a následném rozptýlení nízkoenergiového iontu s atomem přítomným na povrchu vzorku může dojít k jeho neutralizaci. Energie těchto neutrálních rozptýlených částic nese stejnou informaci o prvkovém složení studovaného materiálu jako u částice, která je po odrazu stále v ionizovaném stavu. Zásadní rozdíl je při měření energie a detekci těchto částic a následné interpretaci spekter. Zatímco energie iontů je analyzována pomocí elektrostatického analyzátoru (Electro–Static Analyzer – ESA), energie neutrálů je měřena pomocí jejich doby letu (Time of Flight – TOF). Porovnáním ESA a TOF energiových spekter měřených při stejném rozptylovém úhlu lze získat informace o ionizační pravděpodobnosti, které lze pak použít při simulacích ESA–LEIS spekter. Cílem bakalářské práce bude provedení takových úprav stávajícího zařízení TOF–LEIS, které by umožnily získat spektra při stejných podmínkách jako na zařízení ESA–LEIS (Qtac).

Cíle bakalářské práce:

1. Proveďte úpravy stávající aparatury TOF–LEIS na Ústavu fyzikálního inženýrství, které umožní provést komparativní měření na zařízení Qtac (ESA–LEIS) ve Středoevropském technologickém institutu.
2. Proveďte vyhodnocení takto získaných spekter s cílem zjistit ionizační pravděpodobnost pro čisté kovy.

Seznam doporučené literatury:

Feldman L. C., Mayer J.W.: Fundamentals of Surface and Thin Film Analysis, North Holland, New York 1986, 1-123.

Rabalais J. W.: Low energy ion{surface interactions, John Wiley & Sons, New York 1994.

Woodruff D. P., Delchar T. A.: Modern Techniques of Surface Science, Cambridge University Press 1986, 195-236.

Termín odevzdání bakalářské práce je stanoven časovým plánem akademického roku 2016/17

V Brně, dne

L. S.

prof. RNDr. Tomáš Šikola, CSc.
ředitel ústavu

doc. Ing. Jaroslav Katolický, Ph.D.
děkan fakulty

Abstract

This bachelor thesis is about the overall procedure of the LEIS experiment with the aim to obtain reionization curve: from the construction adjustment of the original SARS set-up, through the construction assembly and electrical plug-in of the apparatus to the energy spectrum measurement of the pure copper sheet with following computation of reionization curve.

Abstrakt

Tato bakalářská práce pojednává o celkovém průběhu LEIS experimentu s cílem získat křivku reionizace: přes konstrukční úpravu původního přístroje SARS, sestavení i elektrické zapojení LEIS vůbec a měření energetického spektra čisté mědi s následným vypočtením reionizační křivky zvláště.

Keywords

LEIS, low-energy ion spectroscopy, reionization, reionization curve

Klíčová slova

LEIS, nízkoenergetická iontová spektroskopie, reionizace, křivka reionizace

STRAPKO, T. Comparative spectral analysis by ESA-LEIS and TOF-LEIS method. Brno: Brno university of technology, Faculty of mechanical engineering, 2017. 32 p. Supervisor Ing. Petr Bábor, Ph.D.

I declare that I wrote my bachelor thesis *Comparative spectral analysis by ESA-LEIS and TOF-LEIS method* on my own, under the supervision of Ing. Petr Bábor, Ph.D., using the literature stated in bibliography.

Tomáš Strapko

I would like to thank my supervisor Ing. Petr Bábor, Ph.D. for his time, priceless advice, patience and goodwill to guide and help me through my entire effort, despite repeatedly asking the same questions or somewhat rough manipulation with experimental assembly.

I also want to thank Ing. Michal Potoček, Ph.D. for his help with electrical plug-in of LEIS, my colleagues Vojtěch Přikryl and Martin Mikula for their help with its assembly.

For spectra evaluation, my thanks goes to my friends Roman Byrtus and Tomáš Fedorko, who uncovered some MatLab nuances not known to me.

I also thank Natália Bačiková for her corrections of grammar, which is essential to make the proper impression of the thesis.

Finally, I would like to thank my parents, who supported and encouraged me for my entire study and without who this thesis would never be written.

Tomáš Strapko

Contents

Foreword

Low-energy ion scattering (LEIS) is the spectroscopic method used to determine the composition of the sample surface. Due to low-energy ions, this method is exceptionally sensitive to the outermost atomic layer of the surface. In this thesis, the most basic aspects of LEIS experiment are discussed, with the aim to obtain the reionization curve.

Chapter 1, THEORY, sums up the most basic information about LEIS, its kinematics, spectra and effects influencing the measurement. Chapter 1 also describes simulation program ITRBS, which is used to simulate LEIS spectra, LEISInt, program for conversion spectra measured in "channels" to energy spectra and last but not least, discuss the reionization process.

Chapter 2, CONSTRUCTION AND ASSEMBLY, states all steps which were necessary to accomplish before actual measurement took place - from adjusting flange for vacuum chamber to entire assembly and electrical plug-in.

Chapter 3, EXPERIMENT, discuss the process of obtaining reionization curve, the aim of this thesis, begins with the measurements of the unclean sample, proceeds with sample heating and sputtering and concludes with clean sample measurements and finally, obtaining reionization curve. Scattered neutrals and ions are measured on the new LEIS set-up at IPE and scattered ions are measured by Qtac detector instrumented in CEITEC.

Chapter 1

THEORY

1.1 Basic information

LEIS[1] is a quasi non-destructive spectral method using ions of noble gasses with energies from 0.5 to 10 keV for quantitative analysis of sample surface, able to penetrate through the outermost atomic layer up to 10 nm, operating in the high vacuum. The advantage of low energy lies in cross-section of ions[2] - it is larger than for high or medium energy ions, so there is higher probability they will collide with atoms on the surface, yet cross-section is still small enough to approximate interactions between ions and surface atoms as binary collisions. This approximation also counts on non-influence of the **matrix effect** - effect describing the influence on measurement from other elements present in the sample, than analysed elements. Due to this fact, analysis of the flat surface is as easy as analysis of amorphous crystals [1].

The overall mechanism of the method is quite simple - accelerated ions of noble gasses (with known energy) hit the surface of the sample, subsequently being scattered to space and then detected by the detector. During scattering, ions lose part of their kinetic energy. Their decreased energy is measured by the detector and from the loss of their kinetic energy during the collision with target atoms the type of atom which the ion was scattered from can be determined.

1.2 Why do ionized noble gasses are used

The noble gasses have two significant advantages for the LEIS method, which will be discussed now, respectively - first, in general, as a neutral atoms, second as an ionized particles[3].

First, the atoms of noble gasses are non-reactive due to their octet (doublet) configuration of valence electrons, means they necessitate not to share their valence electron (electrons) with another atom to create a bond between them. Non-reactivity of these gasses considerably decreases the probability of surface contamination.

[1] low-energy ion scattering

[2] Cross-section scales with $\sim 1/E^2$, where E is **energy of particle**. For lower energies, this scaling is less significant [1].

[3] Usually He^+, Ne^+, Ar^+, Kr^+ are used for LEIS applications.

Second, noble gasses in their ionized state are neutralized with high probability in the case they penetrate under the outermost atomic layer of the surface - effect that, although, occurs for all particles, but for the noble gasses this is especially true, thus these particles will not influence the measured spectrum. On the other hand, particles scattered from the outermost layer will remain positively charged. Of course, penetrated particles frequently gain their positively charged status back before they leave the sample and so appear in the measured spectrum [1].

1.3 Uniqueness of LEIS method

Before the description of LEIS kinematics, it should be made clear, why LEIS is a unique method of surface analysis - after all, HEIS[4] and MEIS[5] are also capable of executing such spectroscopy measurements. That undoubtedly is true, yet both methods require to add shadowing or blocking conditions[6] for the secondary sputtered ions from sample surface are likely to considerably influence measured spectrum. The uniqueness of LEIS lies, again, in low energy - they are no sputtered particles of the sample (most of the times) and because of the noble gas ions behaviour, i.e. high probability of neutralization after penetration and remaining positively charged after being scattered from the top layer, LEIS possesses only information about the surface [1]. Of course, they are some compromising effects to the spectrum in the real experiment. These effects are discussed in 1.8.

[4]high-energy ion scattering
[5]medium-energy ion scattering
[6]Brief discussed in following section.

1.4 Shadowing and blocking

Repulsion forces between atom and ions create so-called **shadow cone**, which incident ions can not reach.

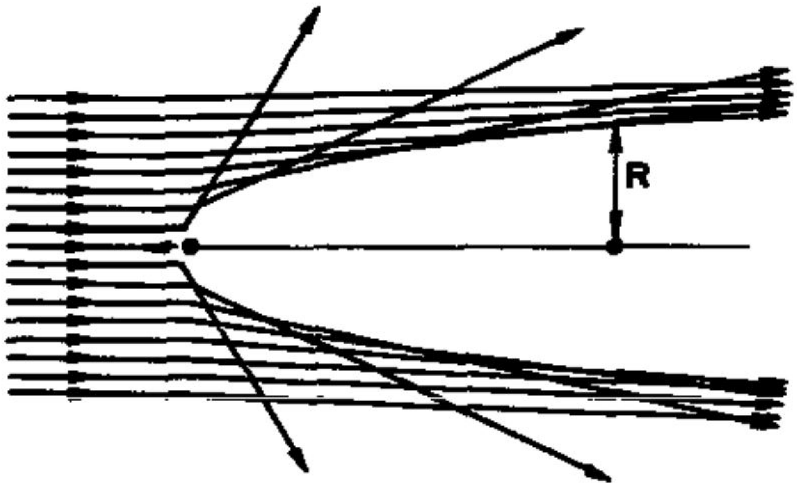

Figure 1.1: Shadow cone behind target atom, acquired from [10].

For Coulombic potential, radius R behind atom in distance d, assuming small angle deflection, is given by

$$R = 2\sqrt{\frac{Z_1 Z_2 e^2 d}{E}} \tag{1}$$

where Z_1 (Z_2) are **atomic numbers of the atom (ion)** and e is **elementary charge** [10].

The exact shape of the cone can be simulated for whatever interaction potential[7]. Deviations from the simulated shape is cause by actual potential's inexactness [2]. If incident ion takes place from subsurface atom, this atom creates a point source emitting particle, causing another, unreachable cone for outgoing ions, called **blocking cone**, with similar blocking mechanism as for shadowing.

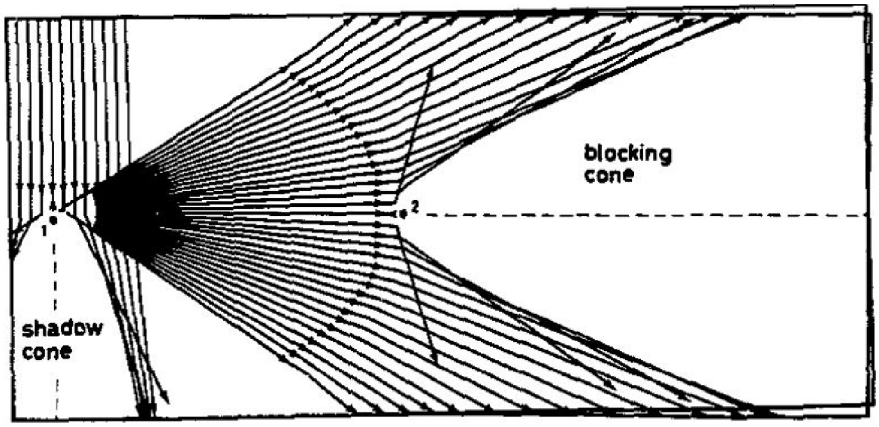

Figure 1.2: Blocking cone behind sputtered subsurface atom - 2, acquired from [10].

[7] See 1.6.2, page 8.

1.5 LEIS spectrum

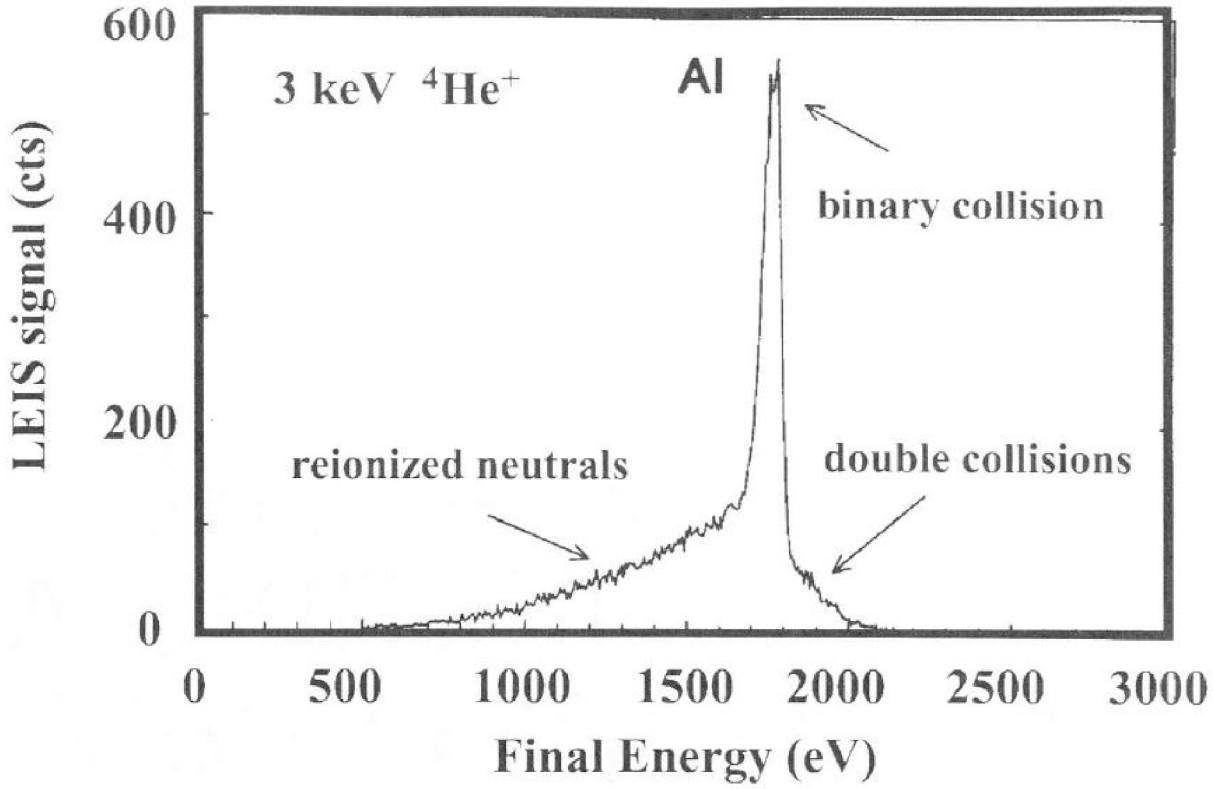

Figure 1.3: Typical LEIS spectrum for pure Al sample with described sections, acquired from [2].

The vertical axis describes counts of scattered ions[8] and the horizontal describes what energy were they scattered with. **Peaks**, i.e. **binary collisions**, represent elements of the outermost atomic layer, while the rest refers to the layers below the surface. It is clear that from the spectrum can not be determined how many atoms is presented in the surface layer (peaks) due to the rest of spectrum. What can be determined is the ratio of coverage by these elements [9].

1.6 LEIS kinematics.

To explain the basic mechanism of interactions between particles, we will discuss now binary collisions more thoroughly.

[8] Or counts per nC, or yield in auxiliary units.

[9] SurfaceLab program for measurement evaluates except-peak spectrum with the full range of elements. Basically, it means that the energy of the scattered ions refers to the situation as if the ions were scattered from corresponding element presented in the surface layer. Obviously, this evaluated spectrum does not contain information about the real composition of layers below surface, i.e. those elements are not really presented in the layer. Program LEISInt, by which the spectrum will be evaluated in this thesis, requires a further step to determine the energy distribution, as discussed in 1.12.

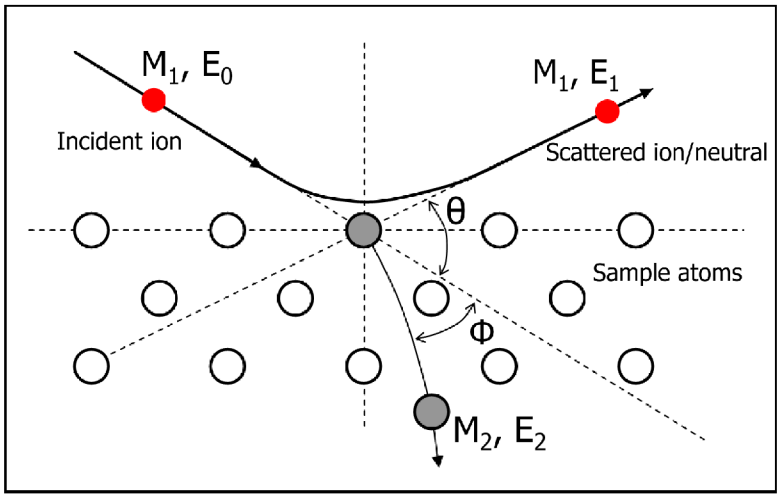

Figure 1.4: Binary collision between the incident ion and sample atom, acquired from [8], modified.

During the process, both kinetic energy and momentum are preserved. From this presumption one equation for kinetic energy is obtained:

$$\frac{1}{2}M_1v_0^2 = \frac{1}{2}M_1v_1^2 + \frac{1}{2}M_2v_2^2 \tag{2}$$

and two equations for momentum, Equation 3 referring to the original direction of accelerated ion, Equation 4 to the direction perpendicular to the original one of the induced ion[10] [4]:

$$M_1v_0 = M_1v_1cos\theta + M_2v_2cos\phi, \tag{3}$$

$$0 = M_1v_1sin\theta - M_2v_2sin\phi. \tag{4}$$

Equation 3 and 4 refer to the complete momentum of binary collision between incident ion and target atom. This equation can be rewritten into more general form

$$\vec{p_0} = \vec{p_1} + \vec{p_2} \tag{5}$$

$\vec{p_0}$ referring to **momentum of the incident ion**, $\vec{p_1}$ to **momentum of the scattered ion** and $\vec{p_2}$ to the **momentum of the target atom**, both after the collision.

The aim is to obtain a general equation for energy of scattered ion depending only on the scattering angle θ and mass ratio between target atom and incident ion.
To achieve that, both $\vec{p_2}$ and angle ϕ have to be eliminated. For this purpose, relocation $\vec{p_1}$ to the left and squaring the equation gives the form

$$p_2^2 = p_0^2 + p_1^2 - 2p_0p_1cos\theta \tag{6}$$

Now, after substitution energy in Equation 2 using formula $E = p^2/2m$ implies the quadratic equation for p_2:

$$p_2^2 = \frac{M_2}{M_1}(p_0^2 - p_1^2) \tag{7}$$

[10]Since the complete derivation for the final equation was not found entirely step-by-step, i.e. only without Eq. 2 and 3 or without following equations for momentum, the whole derivation is stated in this thesis.

and substitute p_2^2 in Equation 6 by this formula. The conclusion is a quadratic equation for p_1:

$$p_1^2\left(1+\frac{M_2}{M_1}\right) - 2p_0p_1cos\theta + p_0^2\left(1-\frac{M_2}{M_1}\right) = 0 \tag{8}$$

and the solution

$$p_1 = p_0\frac{cos\theta \pm \sqrt{r^2 - sin^2\theta}}{1+r}, \tag{9}$$

in term of energy

$$E_1 = E_0\left(\frac{cos\theta \pm \sqrt{r^2 - sin^2\theta}}{1+r}\right)^2, \tag{10}$$

where E_0 and E_1 stands for the **initial** and **final energy of ion**, θ is **scattering angle** and $r = M_2/M_1$ stands for the ratio between the **atom** and **ion mass**.

Solutions for this equation exist only in the case when $M_2 > M_1$, analytically implying LEIS method is unable to detect atoms lighter than currently used ions of noble gas [1]. As an aftermath can be stated that "lighter noble gas is used, wider element spectrum is got". However, this spectrum bears "distinction-inexactness", that is kind of a blur detection of heavier elements, as shown in Figure 1.5. For the more accurate distinction between these, the choice of heavier noble gas is a must: "...from the one who has been entrusted with much, much more will be asked." [5]

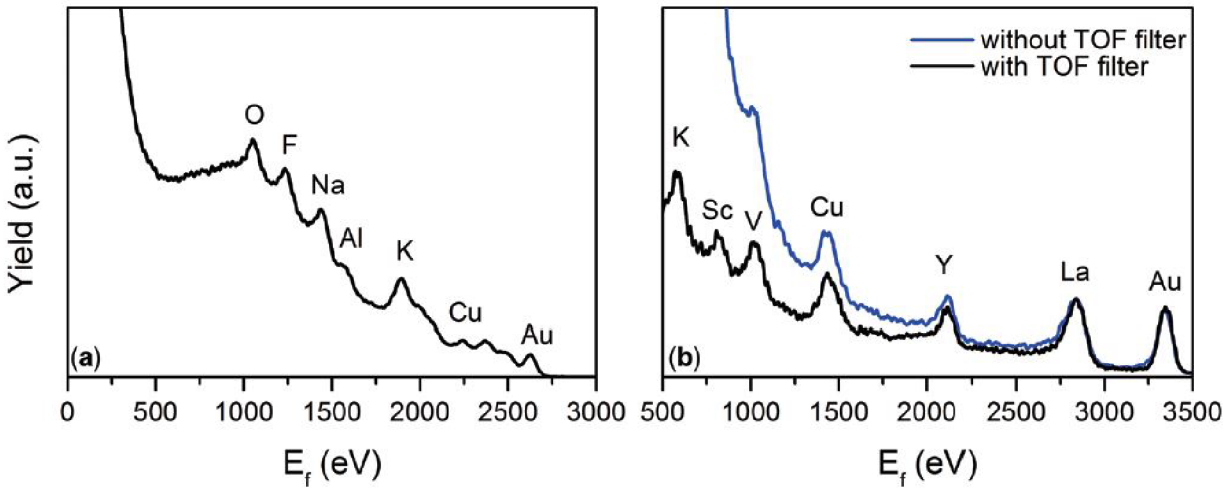

Figure 1.5: 3 keV He^+ (a) and 5 keV Ne^+ (b) distinction of elements. Spectrum for He^+ does not recognize, for example, La[13]and Y[14]between Cu and Au. On the other hand, O, F, Na and Al are contained in He^+ spectrum, opposite to Ne^+ spectrum. Acquired from [1].

Ratio $k = E_1/E_0$ is called **kinematic factor**. Very simple energy-change equation

$$\Delta E = kE_0 - E_0 = E_0(k-1) \tag{11}$$

[14]lanthanum
[14]yttrium

shows that ion energy loss during interaction with the atom of the surface depends only on the mass of both particles and the scattering angle [1, 4].

To obtain maximum efficiency, it is suitable for scattering angle to be set from 120° to 150° and angle between the ion beam and surface trajectory should be smaller than 60°. With this set-up, ions are almost exclusively scattered from the surface atoms. [1]

1.6.1 Thomas-Fermi statistical model of the atom

The Thomas-Fermi statistical model of the atom is named after Llewellyn Hilleth Thomas and Enrico Fermi (who is also known for Fermi-Dirac distribution etc.). Model assumes that pair of electrons with different spin in the atom forms a degenerate gas, i.e. a gas consisting of fermions. Electrons create this pair due to oscillations of the atomic grid (phonons). The model works for a bulk material with numerous atoms and is used to find the distribution of the electron density, for the solution of the Schrödinger's equation for a great number of atoms is difficult.
The procedure for obtaining the general potential consists of finding the formula for the electron density in the distance r from the referential potential φ_0. Next step is substituting this formula for the density in the **Poisson's formula**

$$\Delta\varphi' = -\frac{\rho}{\epsilon_0}. \tag{12}$$

1.6.2 Interaction potential

Between ions and surface atoms occurs no interaction until considering large distances, i.e. dozens of atomic dimensions. In the moment both particles are close enough for their electron clouds to overlap, an overall interaction between both electrons and nuclei of both atoms appears, including electron-electron and both atoms' nucleus-electron interactions. To describe this effects, potential which depends only on distance between nuclei should be found - $V = V(r)$. Due to electron cloud, interaction between nuclei of both atoms are surpassed. Considering this fact, so-called **screening function** $\Phi(r)$ is introduced and the general equation is obtained

$$\Phi(r) = \frac{V(r)}{C/r} \tag{13}$$

where $V(r)$ represents **general potential** between both nuclei and C/r stands for **pure coulombic potential** between nuclei.

The most common way to obtain screening function is by the Thomas-Fermi statistical model of the atom (see above). Empirical screening functions are mostly based on this model.
The whole derivation of the potential between two colliding particles exceeds the scope of bachelor thesis. Only the basic model and the idea behind the complete derivation of the general formula for the potential are described. For more thorough procedure, see [2].
A solution of Eq. 11 (with substituted formula for the potential) give the final equation for the general potential

$$V_\Delta(r) = \varphi - \varphi_0 = \frac{Ze}{r}\Phi\left(\frac{r}{a}\right), \tag{14}$$

where Z is the **atomic number** and a is a **screening parameter**. Several modifications of the screening parameter are being used for the more exact description of the collisions with respect to the both projectile and target electron screening.

What is this chapter supposed to state is, that collision between incident ion and target atom is adequate to the situation of the particle in the central field [15].

The actual experiment, however, does not require any information about $V_{\Delta}(r)$, because scattered particles are detected in the "infinite distance", i.e. much bigger distance than the one in which the electron clouds overlap, thus the potential does not have any effect on the measured spectrum [2].

1.7 Non-destructive method

The actual density of surface atoms is at least 10-times bigger than the yield of the induced ion beam, for example, the beam of He^{+} is smaller than 10^{14} particles per cm^2 [7], thus the damage dealt by them consist of moving every 10th surface atom out of its original position in the sample. LEIS is called "non-destructive method" due to this little damage dealt to the surface, as the contradiction to HEIS, MEIS or even SIMS, which causes a mayhem on the sample. For longer exposition time, the surface would be severely damaged by LEIS as well, i.e. actual surface corrugation would be the result.

1.8 Compromising effects

For successful measurement HEIS or MEIS both require blocking or shadowing conditions for surpassing the contribution to signal from ions sputtered out of the sample surface - effect caused due to high energies of ions. Although LEIS relies on low energy, measured signal is often compromised by secondary sputtered ions represented by so-called **tail**, i.e. the beginning of the spectrum contains a lot of particles.

[15] Repulsion of the incident ion, i.e. its movement in central field, is described by **scattering integral**, topic, which exceeds the needs of this thesis. For more information, see [2].

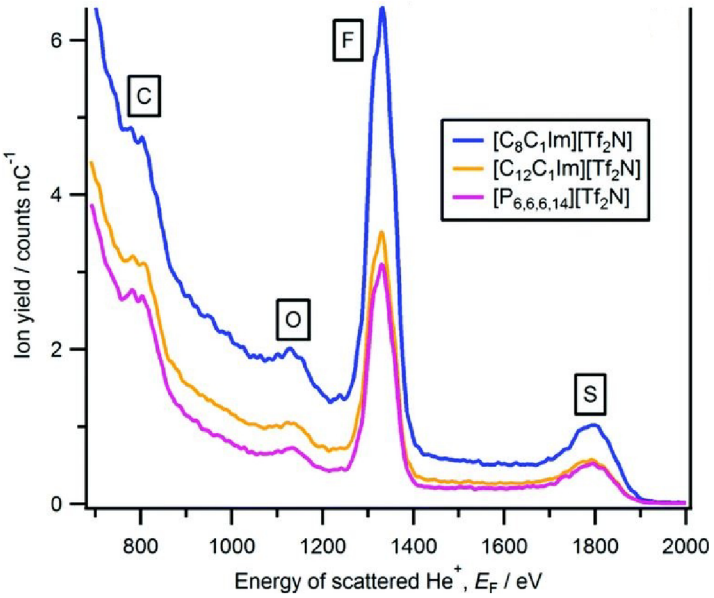

Figure 1.6: Tail, 3 keV He^+, acquired from [11].

However, it does not contradict the statement of non-destructive nature of LEIS. Opposite to sputtered particles by HEIS or MEIS, these mostly do not belong to the outermost layer atoms of analysed sample, but to the impurities presented on the surface sample (oxides etc.). Correction[16] of the signal is executed by both cleaning the sample surface - ion sputtering - or using TOF detector. The spectrum obtained after either of mentioned methods[17] provides more accurate information about surface composition [1].

1.9 Quantitative or qualitative method

At 1.1 is stated that LEIS is a quantitative method. On the other hand, in 1.5 is stated that only obtainable information is about what, not how many of the elements are presented in the outermost layer and their ratio of the coverage. What is then truly meant by the statement in the first chapter?
The answer is, again, the low energy, more precisely the absence of matrix effect, thus measured spectrum can be compared with a well-known bare substrate, oxide, eventually compound. Considering these facts, for an element i in the LEIS signal holds true

$$S_i = S_i^{ref} \frac{N_i}{N_i^{ref}} = S_i^{ref} \xi_i, \tag{15}$$

where N_i^{ref} and N_i are the **atomic surface concentrations** of an element i in the reference and the analysed sample, respectively, S_i^{ref} is the **signal** of the element i in the reference pure sample and ξ_i **surface coverage** by element i [1].

[16] LEIS is able of executing depth-profiling measurements as well, so the spectrum might be influenced by this capability. Since such aspect is not required for the aim of this thesis, it will not be discussed further. For more information, see [1].

[17] See Figure 1.3, page 5.

1.10 TOF detector

TOF[18] detector is a long drift tube usually consisting of deflector plate, an acceleration tube lens and a retarding grid analyser. This set-up allows obtainig four different types of the spectrum [2]:

a)neutrals plus ions (ground potential in the entire tube)
- both ionized and neutral particles hit the detector, only the energy of particles is measured;
b)neutrals only (setting the high voltage on the deflector)
- ions are deflected away from the detector, only neutrals are measured;
c)neutrals and accelerated ions (accelerating voltage on tube lens)
- neutrals and ions are separated due to the difference in their kinetic energy;
d)neutrals and ions with different charges (retarding grid at preselected voltage).

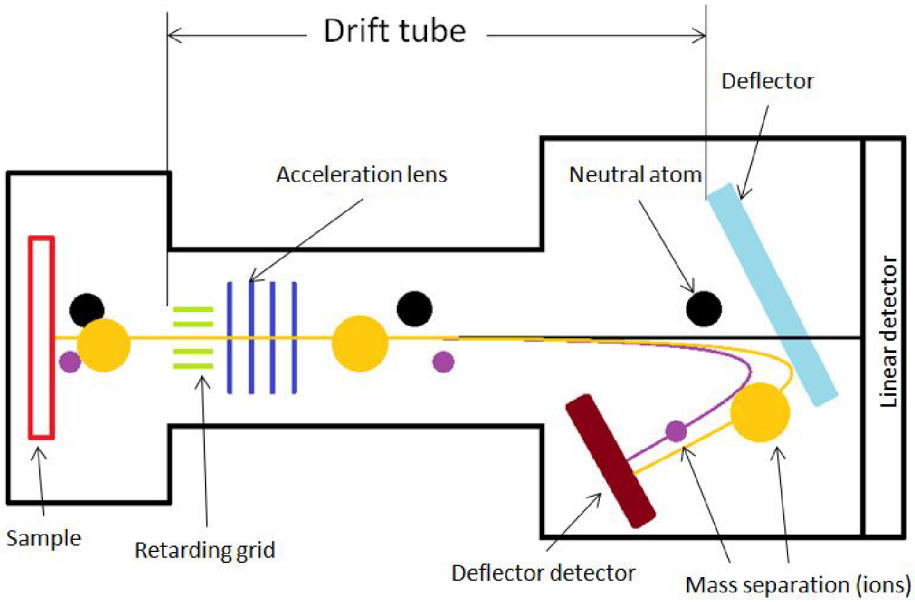

Figure 1.7: TOF detector.

The mass spectroscopy is determined by the energy equation

$$E = \frac{1}{2} M \frac{L^2}{t^2} \tag{16}$$

L representing **the drift tube length**, M **mass of the particle** and t is **the time of flight**. Since L is known, energy E is detected and t is measured, it is easy to determine the mass M [2].

This detector allows to exclude sputtered particles from the sample, i.e. it "removes" tail from LEIS spectrum.

For the own experiment of the thesis, set-up **a** is used.

[18] time-of-flight

1.11 Beam chopping

In order to measure both neutrals and ions - TOF measurement, ion beam must be dosed in pulses, not continually, so the time of flight is measurable.

Beam pulses are achieved with two parallel electrodes - pulsing plates. On the first one, a constant voltage is applied. The voltage on the second one depends on frequency, i.e. the voltage is applied at regular intervals, and the amplitude is the same as for the first electrode. Pulse width normally varies from 5 ns to 100 ns. This way, current that flows through the sample[19] is between 1 nA and 50 nA [2].

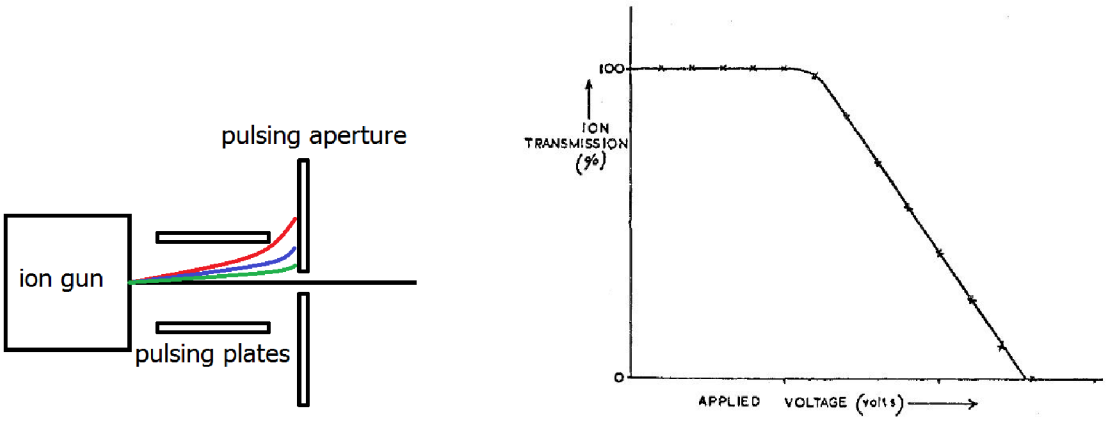

(a) The function of electrodes.

(b) Ion transmission as a function of applied voltage, modified, acquired from[9].

Figure 1.8: Scheme of deflecting system (a) and schematic ion beam dependence on applied voltage (b).

The function of pulsing plates is shown in Figure 1.8, a. Depending on the applied voltage, ion beam either pass through pulsing aperture or is deflected and hit the aperture. Dependence of ion beam transmission on applied voltage is shown in Figure 1.8, b.

[19] For the own experiment, only current<3 nA can flow through the sample.

1.12 LEISInt

LEISInt[20] is a program for evaluation of LEIS spectra. By this program, the own experiment of this thesis will be evaluated.

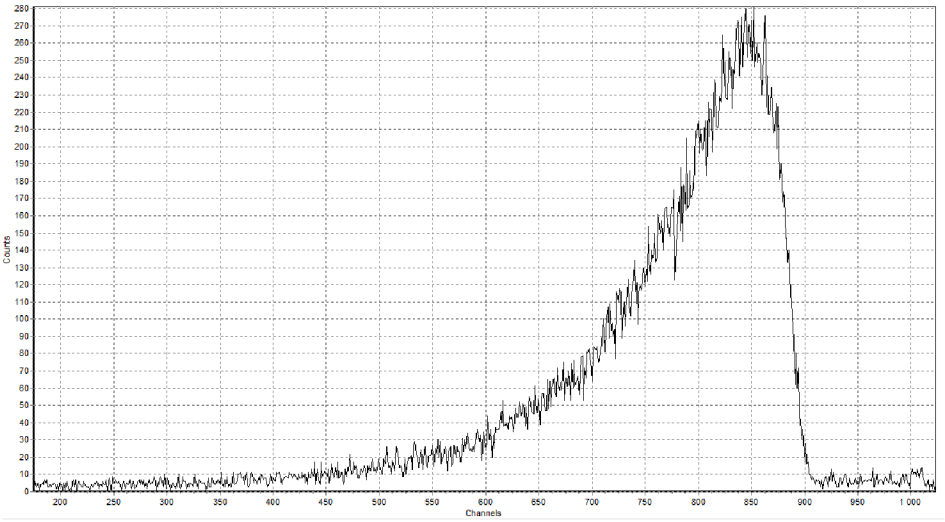

Figure 1.9: Channel spectrum, 3 keV He^+.

The horizontal axis is divided into 1024 channels, vertical axis describes a number of particles impacted on detector [21]. To obtain time-of-flight or energy spectrum, the program requires from user to "get the peak position" of a chosen element, for which the program computes its energy [22].

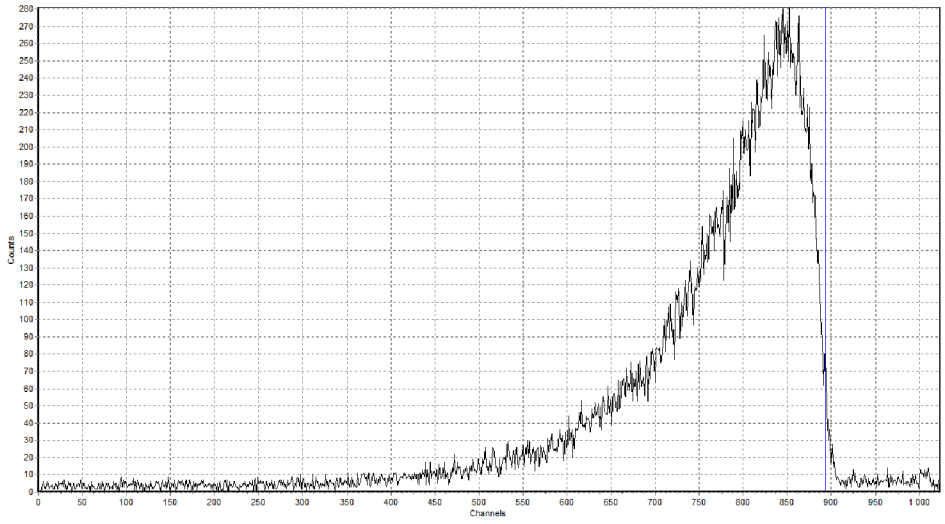

Figure 1.10: Position of the peak determined by the user.

[20] LEIS Integral

[21] Description of the axes is barely visible, but purpose of the picture is just to show output from LEISInt. In 3.1 all spectra are evaluated by Microsoft Excel, with enhanced visibility of the axis' description.

[22] For more details about the program, its computation method and other functions, see [6].

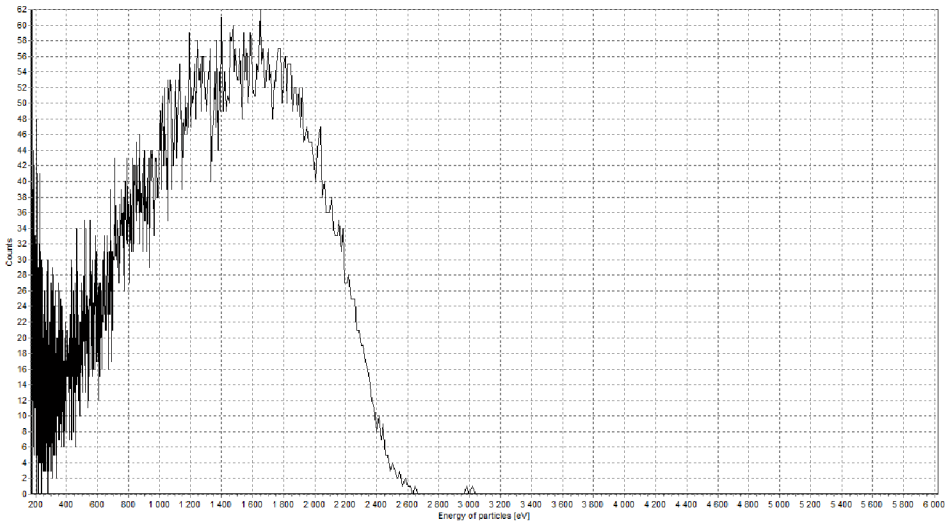

Figure 1.11: Evaluated energy spectrum.

The energy spectrum[23] is significantly noised, as well as, increasing with lower energies, contains particles with higher energy than the energy of incident beam [24]. This error is probably caused by the width of ion pulse, i.e. detector detect some particles from the previous pulse as they were part of a current pulse, so it will evaluate them as particles with much higher energy than 3 keV.

[23]Description of the axes is barely visible, but purpose of the picture is just to show output from LEISInt. In 3.1 all spectra are evaluated by Microsoft Excel, with enhanced scale of the axis' description.

[24]For example, see Figure 3.4 on page 24

1.13 ITRBS

TRBS (Transport Rutheford Backscattering Spectroscopy) is a program for simulation spectrum of particles backscattered from the sample surface. TRBS[25] uses **jellium model** of solid surface - background of negative charge with randomly distributed positive atomic nuclei. It detects particles in the entire azimuthal angle, the same as Qtac[26]. ITRBS can not deal with particles charges, it only deals with their kinematics. This lack of a reliable tool for evaluating spectrum leads to two problems:

1. Any noble gas ion which penetrates the outermost atomic layer will neutralize. The only way to detect such ions is their reionization during the interactions with the surface layer atoms and keeping the charge when they leaving the surface. Reionization probability depends on the energy of ions leaving the surface as well as the surface composition. The task is to find this reionization function for different surfaces.

2. Ions scattered from the outermost atomic layer will remain charged with great probability - this is the reason of peaks in the LEIS spectrum.

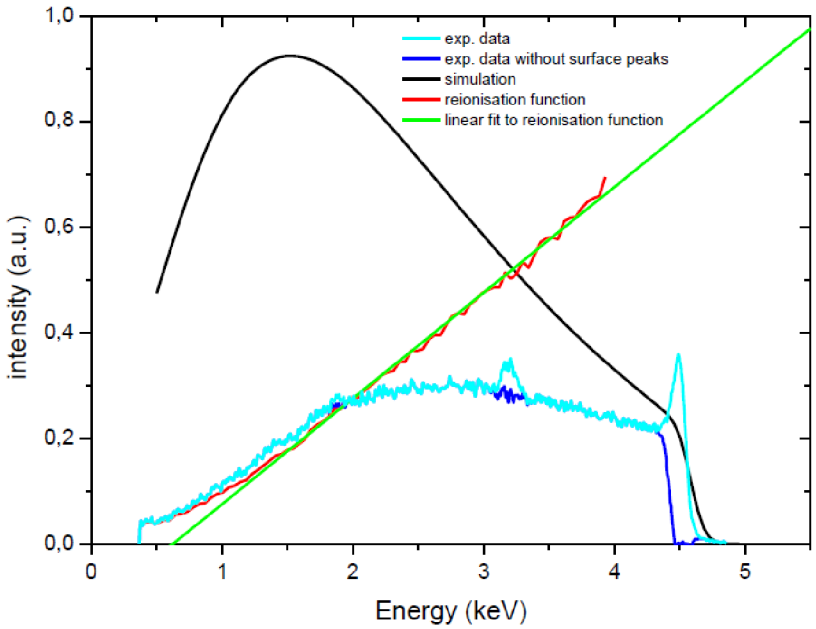

Figure 1.12: Reionization curve, 5 keV He^+ scattering from pure HfO_2, acquired from [3].

To determine reionization curve[27], peaks in experimental spectrum could be simply neglected, for they relate to backscattered ions from the outermost atomic layer, which remain positively charged during the process. Surpassing the peaks, i.e. following the blue line, means to subtract or simply ignore them. Subtracting is suitable for small O peak (around 2 keV) and Cl contamination peak (around 3 keV). The peak of Hf is different - for there is no simple baseline, subtraction is not a useful tool. Unfortunately, there is no suitable method to surpass the peak, it just has to be ignored.

[25] ITRBS is TRBS implemented in IONTOF SurfaceLab software.
[26] See the beginning of 2.1.
[27] The method of obtaining this curve is described in the following chapter.

1.14 Reionization

In the end of the theoretical part of the thesis comes the final explanation, what does reionization process and reionization curve, which both emerged several times in previous chapters, mean.

Reionization process (reionization) is the process during which the ions penetrated under the outermost atomic layer repeatedly loose and gain their ionized state because of multiple interactions with sample atoms. Conclusion is if the scattered ions will remain charged after all the collisions, their energies are subsequently contained in the 'except-peak area' of the LEIS spectrum.

Reionization curve is the curve obtained as a ratio of the ion curve to the curve of both neutrals and ions. It says, how many penetrated ions kept their charge after leaving the sample surface per one scattered particle.

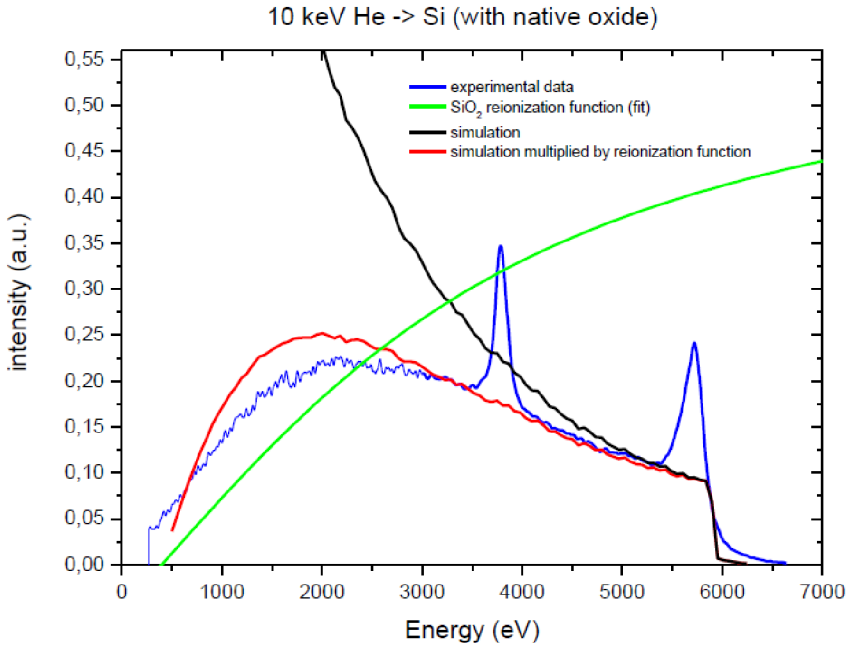

Figure 1.13: Complete solution for a Si sample, acquired from [3].

Reionization begins at threshold energy (hundreds of eV) and below that energy the probability is zero [3].

Nowadays, the study of this curve is intensive, for there is a thought it might posses some information about the layer under the outermost one. Regardless, it is quite new and unexplored area of research.

After all the brief and fundamental theoretical part of the thesis, we can finally move to the thesis's objective, which is to experimentally obtain the reionization curve for the pure metals. Why and how is discussed in the following chapter.

Chapter 2

CONSTRUCTION AND ASSEMBLY

2.1 Motivation

In CEITEC, Brno, LEIS measurements are executed on the pure copper sheet with Qtac detector. This detector collects scattered ions from the whole azimuthal angle under the 35° angle between the ion beam and the analyser.

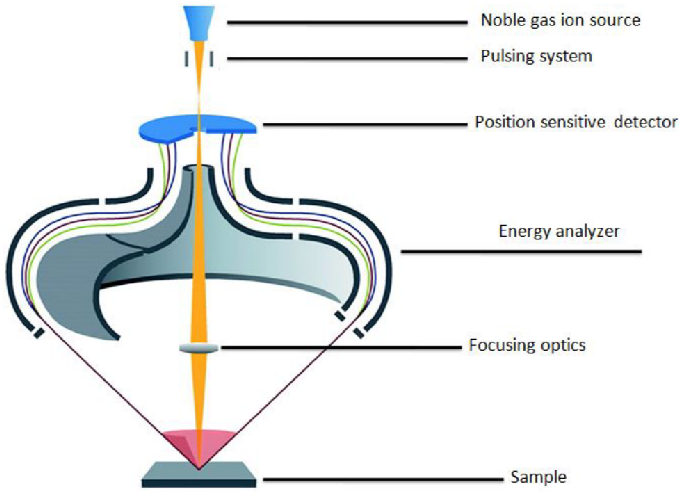

Figure 2.1: Qtac scheme, acquired from [12].

The aim of this thesis is to obtain the reionization curve. Although, to fulfil this task, the spectrum of neutrals must be experimentally measured, instead of reionization curves obtained by divided experimental data by ITRBS simulation. This implies using the TOF detector, which was available in the Institute of Physical Engineering (IPE) as the part of the original layout assembled to detect hydrogen - SARS (scattered and recoil spectroscopy).

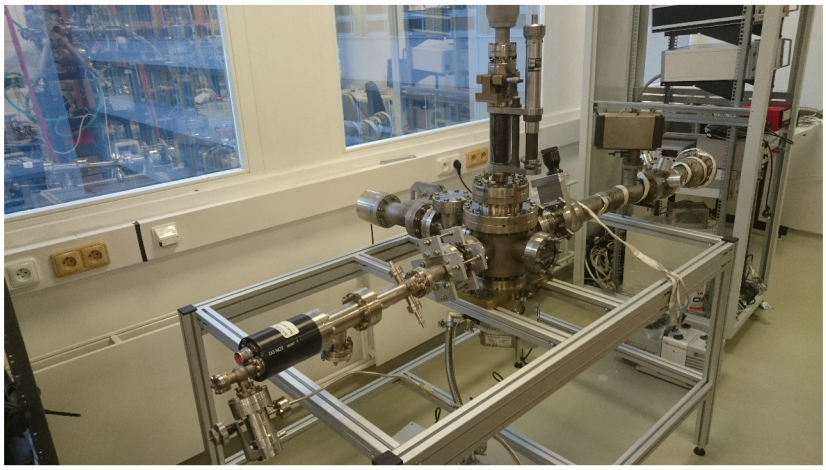

Figure 2.2: SARS on IPE.

The angle between induced ion beam and scattered ions for SARS was only 4°, sufficient angle to sputter the hydrogen from the outermost atomic layer of the sample. Since the possession of TOF detector, the idea of an experimental spectrum, instead of the one simulated by ITRBS, was born. To secure 35° angle between the ion source and the detector was the first task of this thesis to the successful execution of the experiment.

2.2 Solution

The change of current apparatus was to draw a new top flange of the vacuum chamber, which consisted of adjusting the DN160CF flange (a normalized flange for vacuum technology), and that in adding four pipes - first pair (35° angle between their axes) for the ion source and the TOF-LEIS system, second pair (65° angle between their axes) for the second ion source and SIMS detector, the task added as an improvement of entire apparatus. The model and the drawing were both drawn in SolidWorks 2014 program.

Pair of pipes with DN40CF flanges closer to each other is for LEIS set-up, while a pair of more distant pipes is set-up for SIMS. While the 35° angle was a must, the angle for SIMS was adjustable. The original idea was to set the angle at 40°, which occurred to be impossible due to lack of the space near the sample area - both ion sources would collide in this case, for the available LEIS ion source has 35 mm working distance and SIMS ion source requires 40 mm. Considering this fact, the SIMS pipe set-up requires at least 65° between axis.

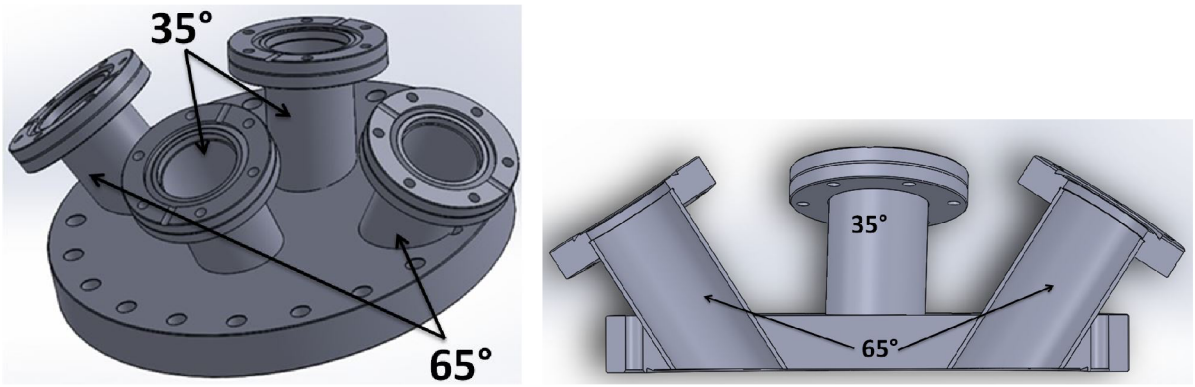

(a) Overall view. (b) Section view.

Figure 2.3: Model of the adjusted flange.

The pipes partially intersect with the holes for the screws, which disables to undergo the usual procedure of securing the flange to the chamber with screws and nuts. Since this is minimal required set-up, the normalized 8.4 mm holes for DN160CF flange were changed to M8x12 inner threads. Nevertheless, this minimal required set-up is also the only possible solution of the problem, since the minimal distance between the inner thread and the inside of the flange is only 0.59 mm. The corresponding distance for holes is 0.57 mm.

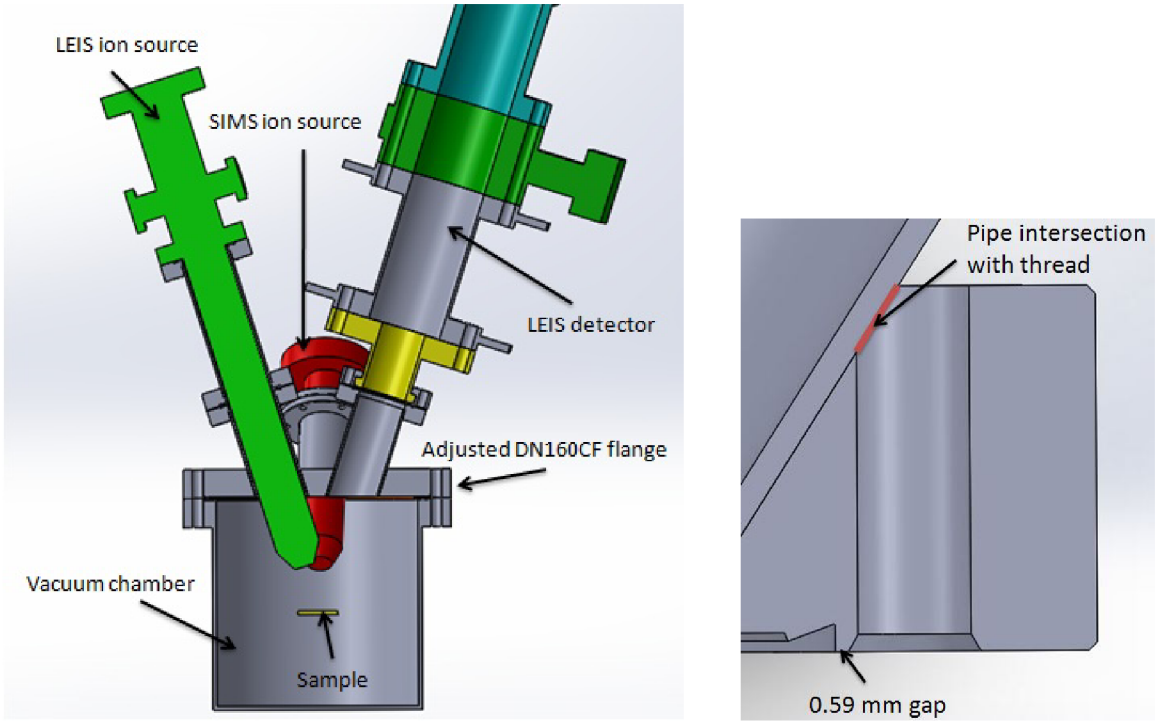

(a) The entire model (except the SIMS detector) for the new assembly.

(b) Detail of the small gap between thread and the inside of the flange.

Figure 2.4: Model section view with the thread detail.

The gap between LEIS and SIMS ion sources is only 1.43 mm, shown in Figure 2.5.

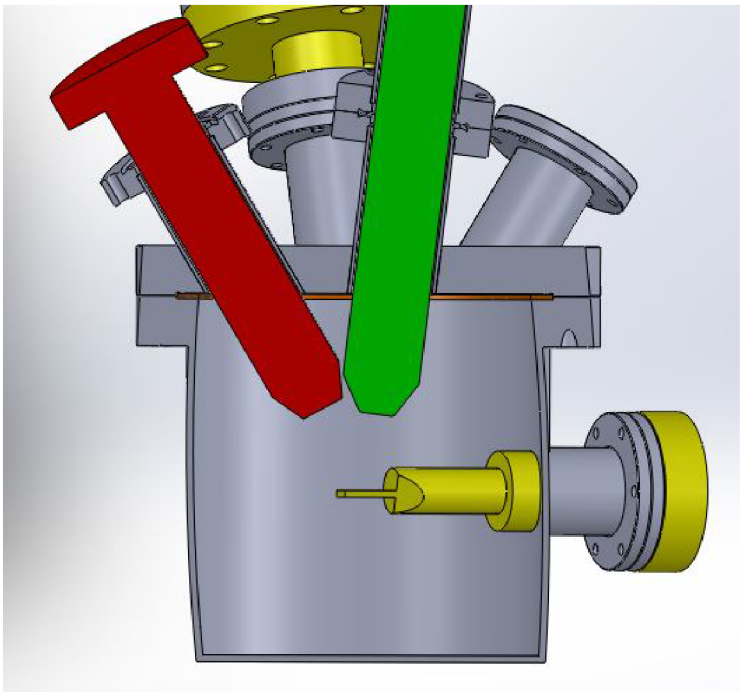

Figure 2.5: Section view of the plane across the both LEIS and SIMS source axis.

Only the sections important for the entire assembly are drawn for each part, i.e. the sections of the parts, in which it had to be decided whether they might collide with other parts or not.

The sheet for the adjusted flange is added in the appendix.

2.3 Assembly

During making process of the adjusted flange, we decided to test the electronics of the entire, yet SARS, system. Since SARS, as well as LEIS, operates in the ultra high vacuum (UHV), that means 10^{-7} Pa and less, the first step was to bake an entire system. During the process, all gas particles trapped in the vacuum chamber and pipes will evaporate and subsequently drain by turbo-molecular pump. The whole assembly was wrapped in the glass-fibre aluminium blanket. The temperature was set to 120° Celsius and baking went on for approximately 24 hours.

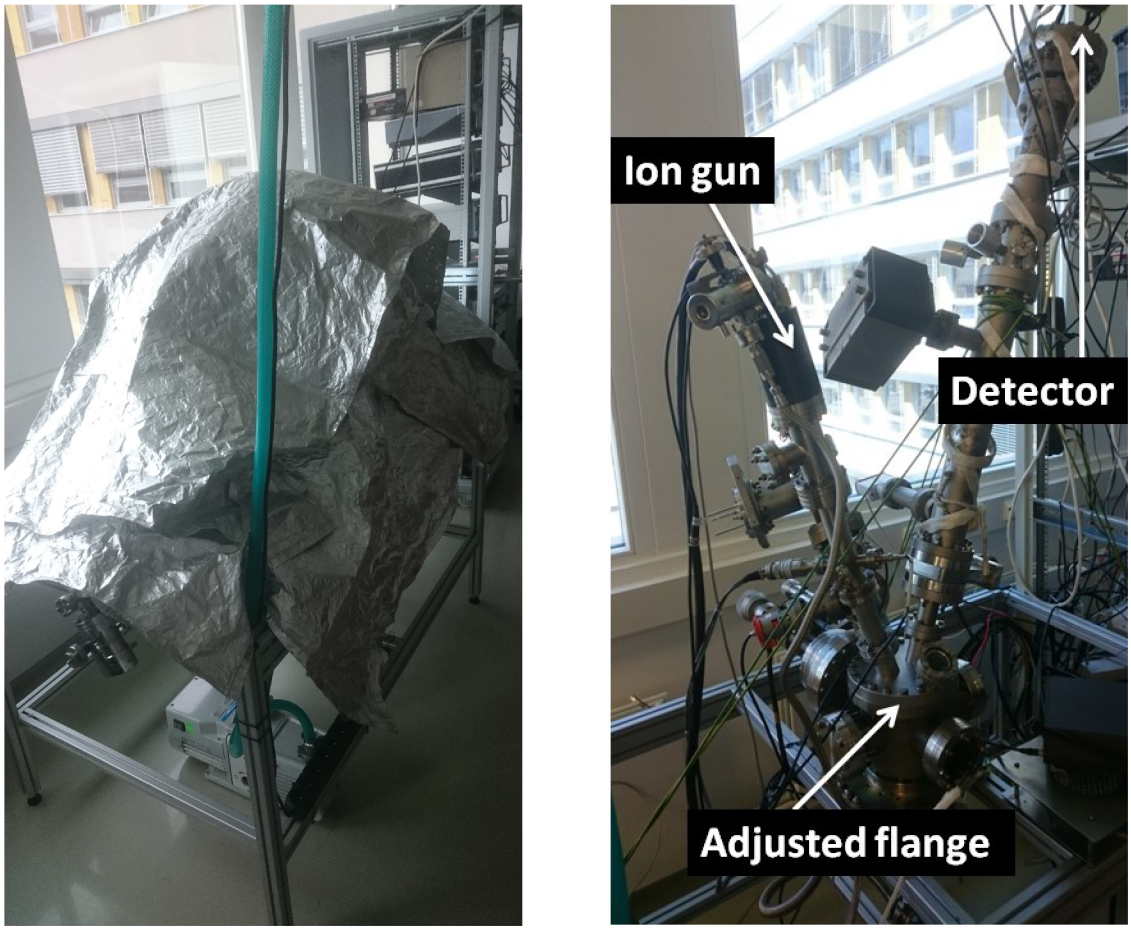

(a) Baking of SARS.

(b) Final LEIS assembly.

Figure 2.6: Baking of SARS wrapped in glass-fibre aluminium blanket (a) and fully assembled and plugged LEIS (b).

After the baking, ion source, detector, PC and other electronics were plugged in and with scattered ions we successfully displayed the sample, thin copper sheet, so we could move on to the final assembly.

Final LEIS assembly is shown in Figure 2.6 The detector is tightened to the frame with strings (temporary solution), otherwise the whole apparatus trembles and that might be destructive for the turbo-molecular pump.

Chapter 3

EXPERIMENT

3.1 Copper oxide

The first experiment was executed for the thin copper sheet with energies 3 keV, 4 keV and 5 keV for exposition time 100 s and 300 s. In this stage of the experiment, the top of the sheet was covered by the native copper oxide [28]

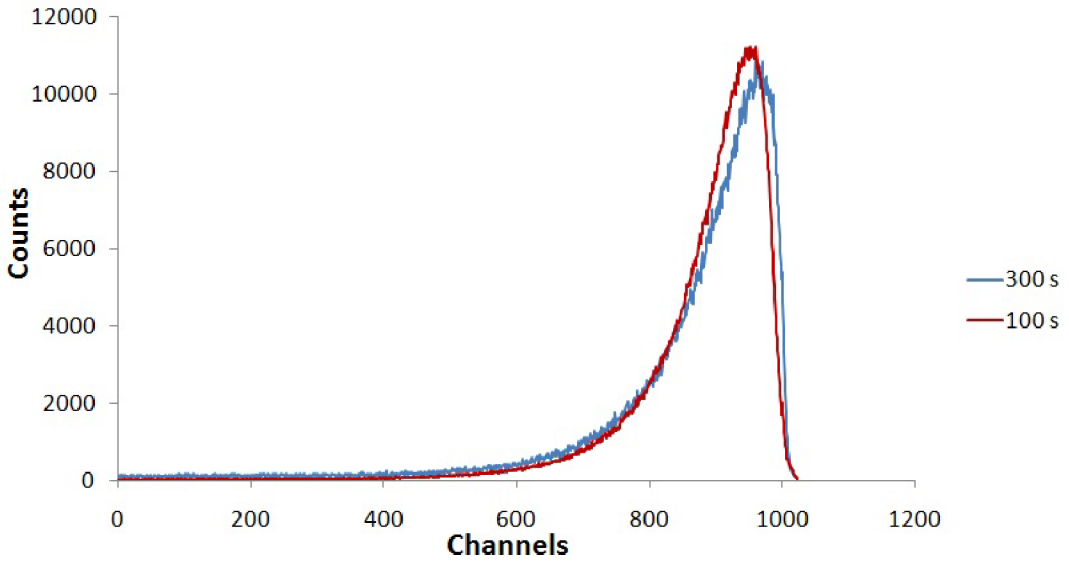

Figure 3.1: 5 keV channel spectrum for 100 s and 300 s exposition time. Spectrum for 100 s was multiplied by 3 for better comparison.

The next step is up to the user to determine the position of the energy peak for sample element. Usually, it is set-up to be in the 1/5th between the channel for maximum counts value and 1024 channel, closer to the second mentioned, in this case around the 1000th channel.

[28] Spectra for 4 keV and 3 keV will not be shown, because they are similar to 5 keV, except "peaks" discussed below.

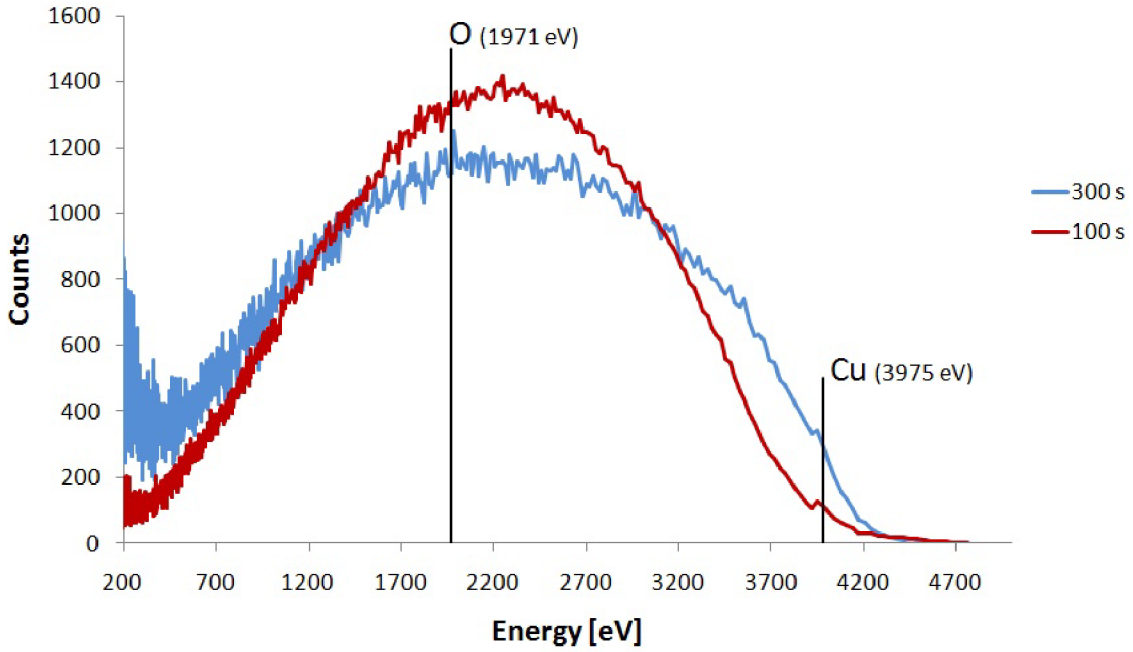

Figure 3.2: Evaluated energy spectrum for copper oxide.

In Figure 3.2, computed energies for both copper and oxygen are marked. To the left from marked copper energy, small peak is visible for 300 s, as well as 100 s spectrum. These peaks might refer to binary peaks for copper, taking into consideration that curves from both sides of peaks are relatively smooth. The gap between marked computed copper energy and its "might-be-peaks" is caused by inevitable inaccuracy in peak determination process mentioned above. The beginning of both spectra, especially for 300 s spectrum, is noised, due to computation from channels to energy spectrum or due to sputtered particles.

3.2 Pure copper

In 2.1 is stated, that LEIS measurements are executed for pure copper sheets. The first step to obtain energy spectrum for the pure copper sheet was to heat the sample. The heating current was set to 1.2 A for approximately 36 hours. Just before measurement, its value was changed several times to 4 A for approximately 10 s to repulse as many impurities from the sample surface as possible.

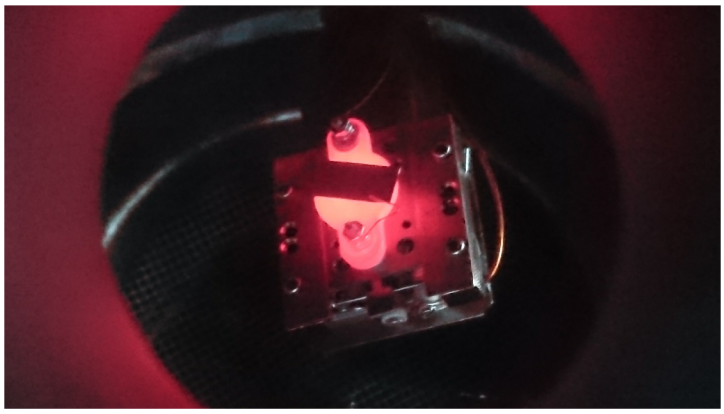

Figure 3.3: Heating of the sample.

Next step was to sputter the sample surface. Ions of He with 5 keV energy were used for approximately 30 minutes exposition time.

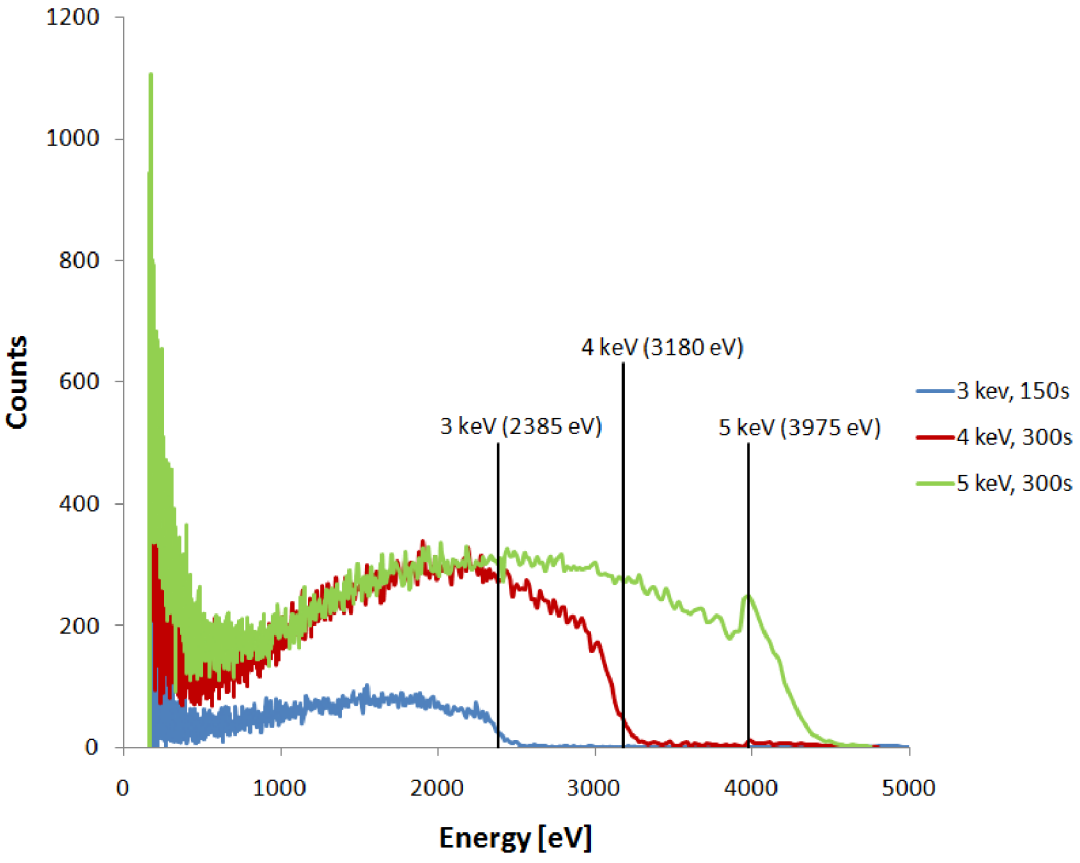

Figure 3.4: Spectra after sputtering with energies of binary collisions.

Then, the sample was sputtered for 6 minutes and under constant heating current 1.24 A, 10-minute measurements for 5 keV, 4 keV, 3 keV and 2 keV He ions were executed, one after another, i.e. no sputtering before each measurement.

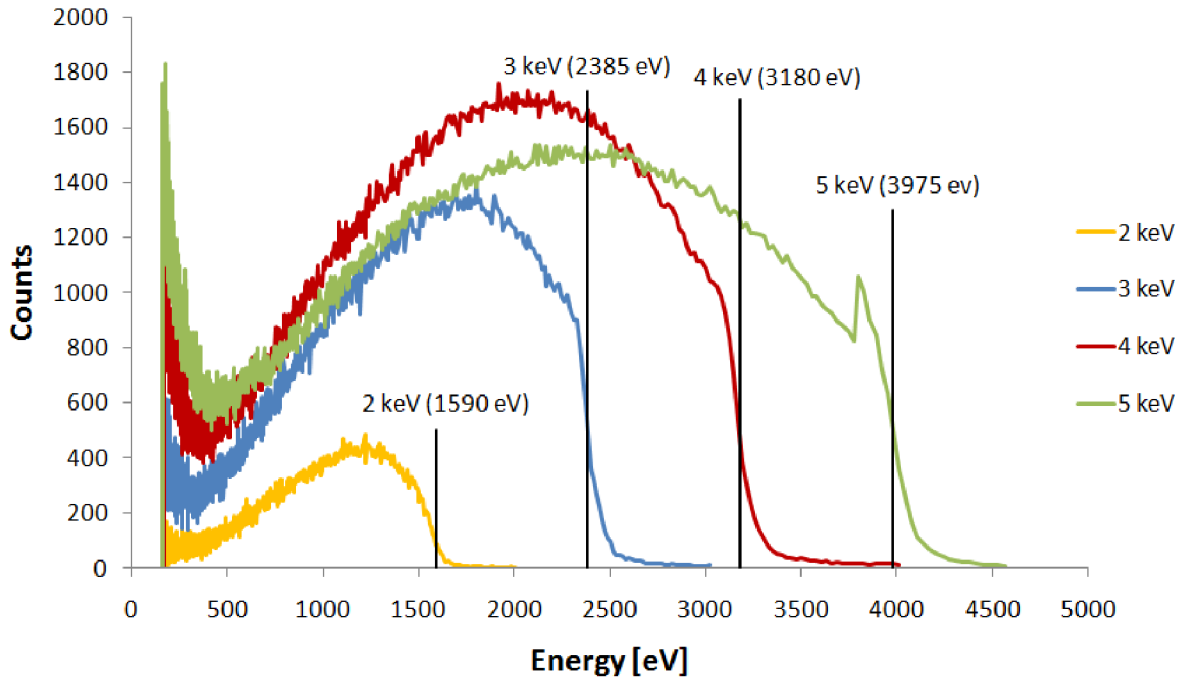

Figure 3.5: Spectra after sputtering with marked energy of binary collisions.

Comparing Figure 3.5 and Figure 3.4, it is clear that longer exposition time provides a stronger signal, i.e. more counts, but has no effect on the signal shape.

Qtac spectra, i.e. ion spectra obtained with incident He^+ beam, for the pure copper sheet in "counts per nC" were obtained by doc. Ing. Stanislav Průša, Ph.D. and with his permission, these are further used.

ITRBS data are in "counts per nC."

Since the TOF data are in "counts", recalculation to "counts per nC" is the next step. Such scale is achieved by:

1. multiplying the average current that flew through the sample[29] by the time of measurement (600 s), so we obtain the electrical charge impacted on the sample in "C" [30];

2. multiplying this number by 10^9, which gives this charge in "nC"c;

3. dividing the TOF spectrum by this number.

[29] In our experiment the corresponding currents that flew through the sample are: 0.09 nA (3 keV), 0.21 nA (4 keV), 0.3 nA (5 keV).

[30] Coulomb.

Now, we have all three spectra in the same units. However, spectrum for ITRBS scales with 10^4, whereas Qtac data scales with 10^2 (10^1, depends on the incident beam energy) and TOF data scales with 10^1. We will, of course, compute reionization curve for this data, but for mutual comparison, we will normalize these data to 1, each respectively, as shown in Figure 3.6. Normalization provides one significant advantage - it surpasses all the inexactnesses, which might occur during recalculations, measurement of the time, current etc.

In Figure 3.6, the thicker curve on certain interval of each spectrum is the interval for which the reionization is computed. These curves were obtained by the least square method, intervals were chosen from the point from which the Qtac spectrum data is only growing to the reasonable point before the peak, so contribution of ions sputtered, as well as scattered from the surface was practically eliminated.

Obtaining[31] the actual reionization curve required one small correction. Since the ITRBS "detector" collects scattered ions from the entire azimuthal angle, its signal is considerably stronger than for the TOF spectrum. To calibrate this effect, reionization curve for ITRBS was multiplied by **correctional factor** 2000, which balances two significant differences between these signals:

1. LEIS detector is approximately 10^{-3}-times smaller than the ITRBS "detector";

2. The **instrumental factor**, i.e. the ratio between detected and impacted particles, for both detectors are different.

[31] The interval for computation are the same as for the normalized spectra, curves are obtained by the least square method as well.

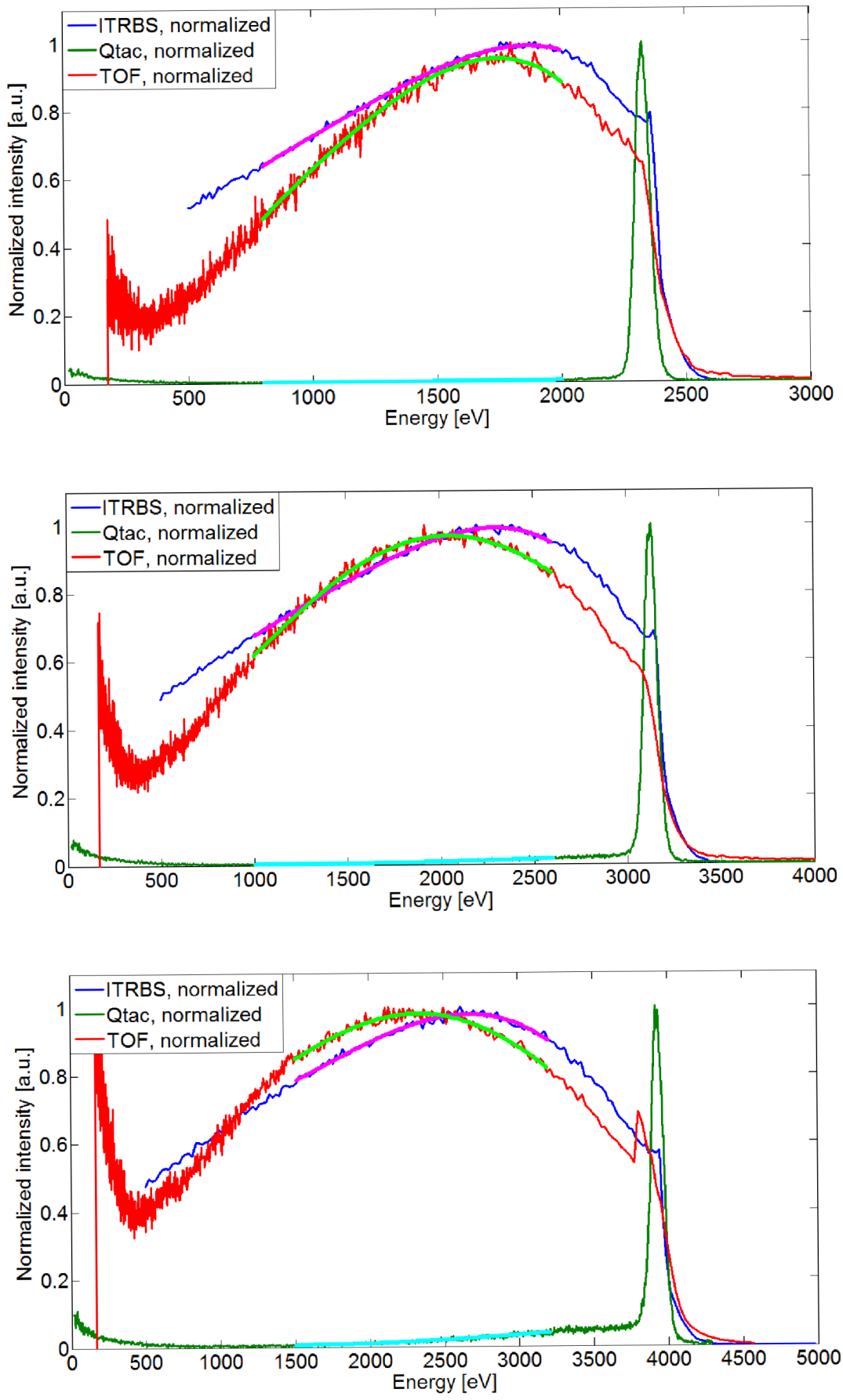

Figure 3.6: Normalized spectra for 3 keV, 4 keV and 5 keV He^+ beam.

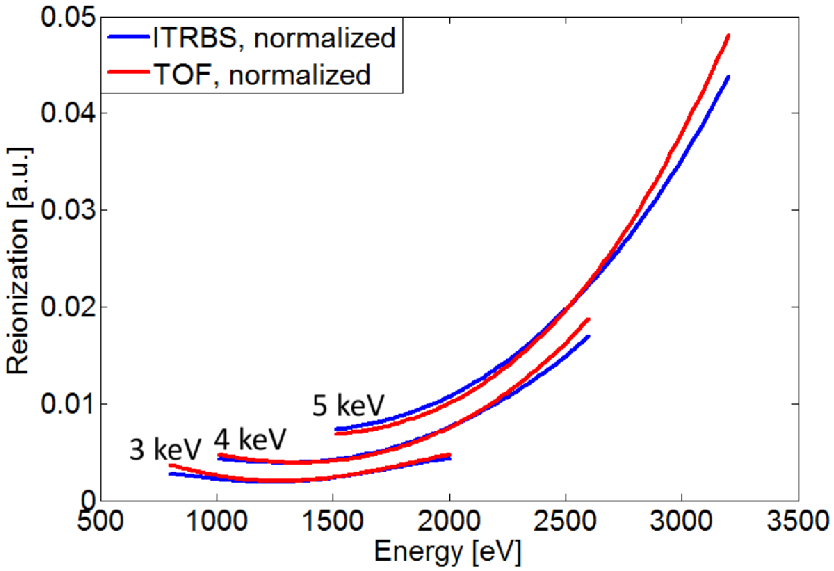

Figure 3.7: Normalized reionization curve.

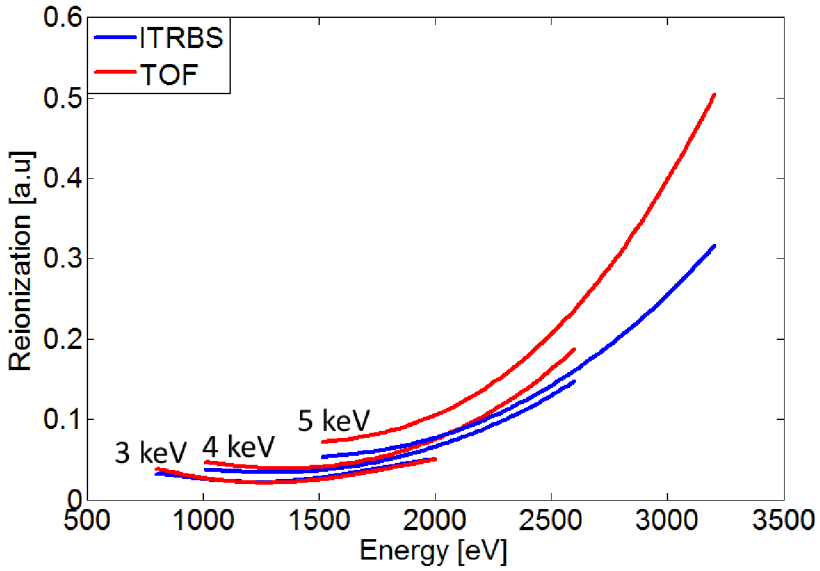

Figure 3.8: Reionization curve.

Normalized ITRBS and TOF spectra, Figure 3.7, show very similar curves for reionization, whilst curves for spectra without normalization, Figure 3.8, show more significant divergence, especially for 5 keV. The curves for 3 keV are, however, almost identical. In the case of these spectra, we must proceed with caution - since the structural factor is not known, correctional factor 2000 might not be the most fitting, therefore divergence between reionization curves for certain energy might be inexact.

Summary

This bachelor thesis was aimed to obtain the reionization curve for the pure copper sheet with the use of LEIS system. This curve informs about how many particles penetrated under the sample surface kept their charges after they left the sample.

The first chapter, THEORY, discussed the basic knowledge about the LEIS, its advantages, limitations, basic principles about atomic collisions as well as a brief summary about TOF detector and importance of beam chopping. In the end were mentioned two programmes, the first - ITRBS - for simulating ions and neutrals spectrum, the second - LEISInt - for evaluating spectra measured by TOF-LEIS on IPE.

The second chapter, CONSTRUCTION AND ASSEMBLY, described all the tasks required to accomplish before the experiment could take a place. Original layout possessing TOF detector was SARS, with scattering angle 4° between incident ion beam and detector. This angle had to be changed to 35°, the same angle as the Qtac detector collect scattered particles from, which was achieved by the construction of the new flange, securing this angle. The last part was to plug-in the entire system.

In the third chapter, EXPERIMENT, is explained how the measurements were executed and how the reionization curve was obtained. The divergence between reionization curves for ITRBS and TOF spectra is increasing with higher energies. This effect is more significant for the reionization curves without previous normalization, although due to the uncertainty of correction factor, it must be considered with caution. For this reason, normalized spectrum seems to be more valuable. In conclusion, we might say, that ITRBS and TOF measurements provide similar curves.

Appendix

The sheet for the adjusted flange is originally in the size of A3, here it is added in scale 1 : 2, i.e. on the A4 paper.

The drawing of adjusted flange is written in the Czech language because it was made by Czech company Vacuum Praha. Translation of used notes:
"Redukce LEIS" - reduction LEIS;
"ostatní díry dle normy pro DN160CF" - other holes with respect to the norm for DN160CF.

List of Figures

Bibliography

[1] BRONGERSMA, H. H. *Characterization of Materials*. J. Wiley & Sons, 2012. 2. edition. DOI: 10.1002/0471266965.

[2] RABALAIS, J. Wayne. *Principles and Applications of Ion Scattering Spectrometry: Surface Chemical and Structural Analysis*. 2002. ISBN: 978-0-471-20277-6.

[3] IONTOF. *ITRBS Tutorial*. SurfaceLab.

[4] ALFORD, T. L., FELDMAN, L.C., MAYER, J. W. *Fundamentals of Nanoscale Film Analysis*. Springer US, 2007. ISBN: 978-0-387-29260-1.

[5] Bible, *Lk 12:48*.

[6] DUDA, R. *Ultrathin film analysis by SIMS and TOF-LEIS* [online]. Brno. Brno university of technology, Faculty of mechanical engineering, 2015 [cited 6.5.2017]. Retrieved from: http://hdl.handle.net/11012/15415.

[7] BART, J. C. J. *Plastics Additives: Advanced Industrial Analysis*. IOS Press, 2006. ISBN: 1-58603-533-9.

[8] Schematic diagram of ion-surface atom binary collision model [online]. The university of Warwick, Department of physics [cited 6.5.2017]. Retrieved from: https://www2.warwick.ac.uk/fac/sci/physics/current/postgraduate/regs/mpags/ex5/techniques/structural/ionscattering/.

[9] JACKSON, P. F. S., WHITEHEAD, J., VOSSEN, P. G. T. *Use of an ion beam chopper for improved precision in spark source mass spectrography*. In: *Analytical Chemistry*. 1967, **39**(14), 1737-1742. DOI: 10.1021/ac50157a035.

[10] STENSGAARD, I. *Surface studies with high-energy ion beams*. In: *Reports on Progress in Physics*. 1992, **55**(7), 989-1033. DOI: 10.1088/0034-4885/55/7/003.

[11] VILLAR-GARCIA, I.J., FEARN, S., DE GEORGIO, G. F. et al. *The ionic liquid-vacuum outer atomic surface: a low-energy ion scattering study*. In: *Chemical Science*. 2014, **5**(11), 4404-4418. DOI: 10.1039/C4SC00640B.

[12] CUSHMAN, C.V, BRUNER, P., ZAKEL, J. et al. *Low energy ion scattering (LEIS). A practical introduction to its theory, instrumentation, and applications*. In: *Analytical Methods*. 2016, **8**(11), 3419-3439. DOI: 10.1039/C6AY00765A.